APPLIED AND ENVIRONMENTAL MICROBIOLOGY, Oct. 1997, p. 4039–4046 Vol. 63, No. 10
0099-2240/97/$04.00+0

Hydrogen Concentration Profiles at the Oxic-Anoxic Interface: a Microsensor Study of the Hindgut of the Wood-Feeding Lower Termite *Reticulitermes flavipes* (Kollar)

ANDREA EBERT AND ANDREAS BRUNE*

Fakultät für Biologie, Mikrobielle Ökologie, Universität Konstanz, 78457 Konstanz, Germany

Received 31 March 1997/Accepted 7 August 1997

Molecular hydrogen is a key intermediate in lignocellulose degradation by the microbial community of termite hindguts. With polarographic, Clark-type H_2 microelectrodes, we determined H_2 concentrations at microscale resolution in the gut of the wood-feeding lower termite *Reticulitermes flavipes* (Kollar). Axial H_2 concentration profiles obtained from isolated intestinal tracts embedded in agarose Ringer solution clearly identified the voluminous hindgut paunch as the site of H_2 production. The latter was strictly coupled with both a low redox potential ($E_h = -200$ mV) and the absence of oxygen, in agreement with the growth requirements of the cellulolytic, H_2-producing flagellates located in the hindgut paunch. Luminal H_2 partial pressures were much higher than expected (ca. 5 kPa) and increased more than threefold when the guts were incubated under a N_2 headspace. Radial H_2 concentration gradients showed a steep decrease from the gut center towards the periphery, indicating the presence of H_2-consuming activities both within the lumen and at the gut epithelium. Measurements under controlled gas headspace showed that the gut wall was also a sink for externally supplied H_2, both under oxic and anoxic conditions. With O_2 microelectrodes, we confirmed that the H_2 sink below the gut epithelium is located within the microoxic gut periphery, but the H_2-consuming activity itself, at least a substantial part of it, was clearly due to an anaerobic process. These results are in accordance with the recently reported presence of methanogens attached in large numbers to the luminal side of the hindgut epithelium of *R. flavipes*. If the oxygen partial pressure was increased, O_2 penetrated deeper and H_2 production was suppressed; it ceased completely as soon as the gut was fully oxic. In experiments with living termites, externally supplied H_2 (20 kPa) stimulated methane formation five- to sixfold to 0.93 μmol (g of termite)$^{-1}$ h^{-1}, indicating that the methanogenic activity in *R. flavipes* hindguts is not saturated for hydrogen under in situ conditions. This rate was in good agreement with the H_2 uptake rates exhibited by isolated hindguts, which would account for more than half of the CH_4 formed by living termites under comparable conditions.

The digestion of lignocellulose by termites has fascinated several generations of biologists. Cleveland (9) recognized very early that the basis for the dietary exploitation of wood, at least in the (phylogenetically) lower termites, is a symbiotic association with intestinal cellulolytic protozoa. The symbionts, mainly large, oxygen-sensitive flagellates, are harbored in the so-called paunch, a voluminous dilatation of the anterior hindgut (Fig. 1), together with a numerous and diverse bacterial microflora (for a review, see references 2, 4, and 16). About 15 years later, Hungate discovered the biochemical nature of this symbiosis (17, 18). He postulated that the principal metabolic activities of the protozoa are the depolymerization of polysaccharides and the fermentation of the soluble carbohydrates (e.g., glucose) to produce mainly acetate, H_2, and CO_2. The termite profits from the microbial fermentation products, since it utilizes acetate as its major carbon and energy source. In return, the host comminutes the wood material to a particle size that can be phagocytized by the symbionts, providing them with food and a favorable niche in an otherwise hostile environment. This situation engages both partners in a truly mutualistic symbiotic association (19).

Many years later, Breznak and coworkers discovered that prokaryotic activities also play a significant role in termite gut metabolism. Gut homogenates of most wood-feeding termites show high activities of H_2-CO_2 homoacetogenesis, which may account for as much as one-third of the respiratory requirement for acetate in *Reticulitermes flavipes* (5). Many termite species from other, mainly soil-feeding and fungus-cultivating taxa, however, form substantial amounts of methane (1). Interestingly, H_2-dependent homoacetogenesis and methanogenesis apparently occur simultaneously in most termites, albeit at different activity levels (1). To date, this phenomenon has not been satisfactorily explained, although several hypotheses suggest circumstances under which homoacetogenic bacteria could outcompete methanogens for H_2 (3).

Quite recently, it became apparent that termite hindgut ecosystems are even more complex than this refined model suggested. Brune et al. (6) showed that the hindguts of wood-feeding, lower and higher termites maintain their anoxic status only because of intense oxygen consumption by the hindgut microbiota. This process generates steep oxygen gradients between the oxic gut epithelium and the anoxic center which render the peripheral gut regions microoxic. Leadbetter and Breznak (23) demonstrated that the layer of prokaryotes covering the hindgut wall of *R. flavipes*, a locality that is definitely exposed to oxygen (6), contains a large number of methanogens. These researchers obtained several isolates which seem physiologically adapted to exposure to oxygen and described them as new species of the genus *Methanobrevibacter*, *M. cuticularis* and *M. curvatus* (23). Recent results from our group (36) confirmed that the utilization of oxygen is common among the numerically prevalent members of the cultivable gut microflora of *R. flavipes*. Taken together, these findings support

* Corresponding author. Mailing address: Fakultät für Biologie, Mikrobielle Ökologie, Universität Konstanz, Fach M 654, 78457 Konstanz, Germany. Phone: 49-7531-88-3282. Fax: 49-7531-88-2966. E-mail: Andreas.Brune@uni-konstanz.de.

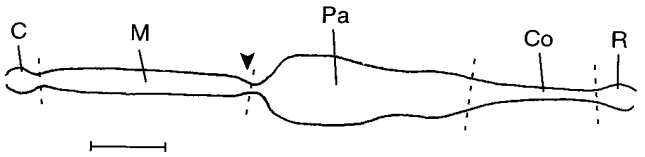

FIG. 1. Schematic diagram of a dissected *R. flavipes* gut drawn in its unravelled state, illustrating the differentiation into crop (C), midgut (M), paunch (Pa), colon (Co), and rectum (R). The arrowhead indicates the insertion point of the Malpighian tubules, which represents the border between midgut and hindgut. Bar, approximately 1 mm.

the emerging concept that the termite hindgut is not a simple, anoxic fermenter, but an axially and radially structured, heterogeneous system characterized by steep gradients of metabolites. New, important questions arise, regarding the intestinal hydrogen concentrations and corresponding H_2 gradients within the gut, the spatial arrangement of the microbial populations that contribute to intestinal hydrogen metabolism, and the fate of the methane formed by such an abundance of methanogens situated directly below the gut epithelium.

In the present study, we report on the determination of radial and axial hydrogen concentration profiles in the gut of the lower, wood-feeding termite *R. flavipes* and the correlation of these profiles with the respective oxygen concentration gradients and intestinal redox potential profiles. The experimental setup was based on that described previously for oxygen gradient measurements (6) but was improved to allow exposure of the guts to defined atmospheres of various compositions during measurement. In addition, we reinvestigated the gaseous emissions of whole termites from this species (27), including the influence of changes in atmospheric hydrogen partial pressures on these activities.

MATERIALS AND METHODS

Termites. Undifferentiated worker larvae (beyond the third instar) were taken from a laboratory colony of *R. flavipes* (Kollar) (Isoptera: Rhinotermitidae) which was originally collected near Dansville, Mich., in 1993 and has since been maintained on a diet of birchwood (*Betula pendula* Roth) and water. For defaunation, termites were subjected to a hyperbaric oxygen treatment (2.5×10^5 Pa of O_2 for 100 min) and then fed a diet of starch for several days. This treatment is known to kill all the larger, cellulolytic flagellates in the hindgut of *R. flavipes*, although the termites remain alive for weeks afterwards (9). The efficient removal of the cellulolytic flagellates was verified by light microscopic examination of the hindgut contents.

Hydrogen and oxygen microelectrodes. Both types of microelectrodes had tip diameters of 10 to 15 μm. Clark-type O_2 microelectrodes with guard cathodes (30) were constructed in our laboratory and calibrated as described (6). Polarographic H_2 microelectrodes had the same basic design but received an anodic polarization (37), an acidic electrolyte of 1 M KCl dissolved in 1 M HCl (38), and the working electrode was coated with platinum black. Prior to platinization, anode tips were cleaned by immersion in acetone and aqua regia (1 min each). They were then electroplated in a solution of 10 mg of hexachloroplatinic acid (Aldrich) in 0.5 ml of lead acetate solution (0.02% [wt/vol]) at a current of about 100 to 500 nA until a microscopically visible coat of platinum black had formed (about 30 to 60 s). Between all steps, tips were rinsed in distilled water (1 min). Preconditioning the electrode surface by a rapidly alternating polarization voltage, as recommended for polarographic H_2 macroelectrodes (21, 37), did not improve its performance.

Testing and calibration procedure. Testing of H_2 microelectrodes was routinely performed by immersing the freshly filled, polarized electrodes in a calibration chamber filled with deionized water which continuously bubbled with the respective gases. During the measurements, the microelectrodes were calibrated while mounted within the glass bell (see below), which was flushed continuously with the respective gas phases. The electrode signal was routinely tested under N_2, air, and a gas mixture of 5% (5 kPa) H_2 in N_2. Other mixing ratios of H_2 with N_2, air, or O_2 were made up with calibrated flow meters with needle valves and checked by gas chromatography. All gases were supplied by SWF, Friedrichshafen, Germany, and were 99.999% pure, except CO and CH_4, which were 99.997 and 99.95% pure, respectively, CO_2, which was 99.95% pure (AGA Gas, Hamburg, Germany), and compressed air, which was provided in-house.

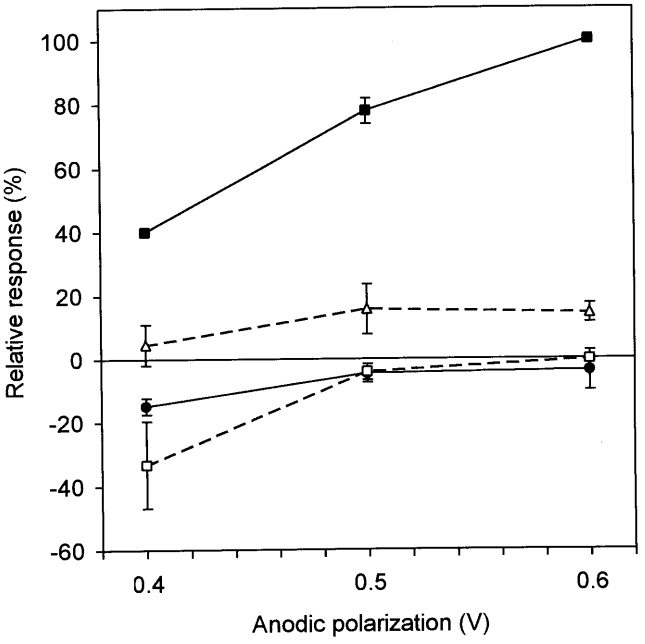

FIG. 2. Relative response of hydrogen microelectrodes to a headspace partial pressure of 5 kPa of H_2 (■) and to the same concentrations of CO (△), CH_4 (●), and O_2 (□) at different polarization voltages. The graph shows averages ± SDs for three different microelectrodes whose absolute responses ranged between 20 and 50 pA (5 kPa of H_2, U_p = +0.6 V). N_2 was used as inert gas in all cases, and the respective background current at each polarization value was subtracted.

Hydrogen microelectrode characteristics. The response to 5 kPa of H_2 ($\cong 10^{-3}$ atm) was typically between 20 and 100 pA, with 90% response times in the range of 5 to 10 s or less. Microelectrodes with higher currents were discarded since they consumed too much H_2 and were usually quite sensitive to stirring (>2%). Electrode response was linear up to 10 to 20 kPa H_2; the individual linearity range differed with the particular electrode. At higher concentrations, the sensitivity of H_2 microelectrodes decreased, whereas oxygen microelectrodes gave a linear response up to hyperatmospheric O_2 partial pressures. Baseline drift and response were sufficiently stable during the measurements, but the general performance of H_2 microelectrodes never reached that of polarographic O_2 microsensors; frequent calibrations were performed throughout the measurements.

The residual currents of individual electrodes differed significantly and were quite often in a direction opposite to that of the electrode polarization (15). Since this phenomenon was invariably linked to an increased cross-sensitivity of the electrode towards O_2, the polarization voltage (U_p) was adjusted until a slightly positive residual current (5 to 10 pA) was achieved. At this point, O_2 cross-sensitivity became negligible (<2%) or the electrode was discarded. H_2 microelectrodes were significantly cross-sensitive to both CO and CH_4 (Fig. 2). The cross-sensitivities (U_p = +0.5 to +0.6 V) were 10 to 20% for CO and less than 10% for CH_4, compared to the signal caused by an identical H_2 concentration. The addition of CO always led to a positive signal, whereas CH_4 diminished the electrode response. CO_2 cross-sensitivity was negligible (<2%) due to the acidic buffering of the electrolyte, as reported by Witty (38).

Measurements. The experimental setup used for microelectrode measurements in termite guts was essentially the same as that described previously (6). After dissection of the termites, the guts were embedded within a microchamber in a gel made up of 1% agarose in insect Ringer's solution. In this study, the chamber was constructed from microscope slides and coverslips, both held vertically but separated from each other by three PVC spacers (each 4 mm thick) which formed the chamber sides and bottom. The chamber was 10 mm high and 25 mm wide. A fresh termite gut was placed flat and fully extended onto a 2- to 4-mm-thick agarose layer at the bottom of the microchamber and quickly covered with an identical layer of molten agarose (40°C), which cooled and solidified immediately. To achieve symmetrical concentration profiles, the PVC spacer at the microchamber bottom could be removed, thus exposing the agarose-embedded gut to the surrounding atmosphere both at the top and bottom of the microchamber in a more or less symmetrical manner.

For experiments under a controlled gas headspace, a glass bell was placed over the microchamber (inverted membrane filtration funnel; Sartorius, Göttingen, Germany), and the top (ground glass surface) was covered with a PVC plate. This cover had an opening formed by a small vertical tube with an inner diameter

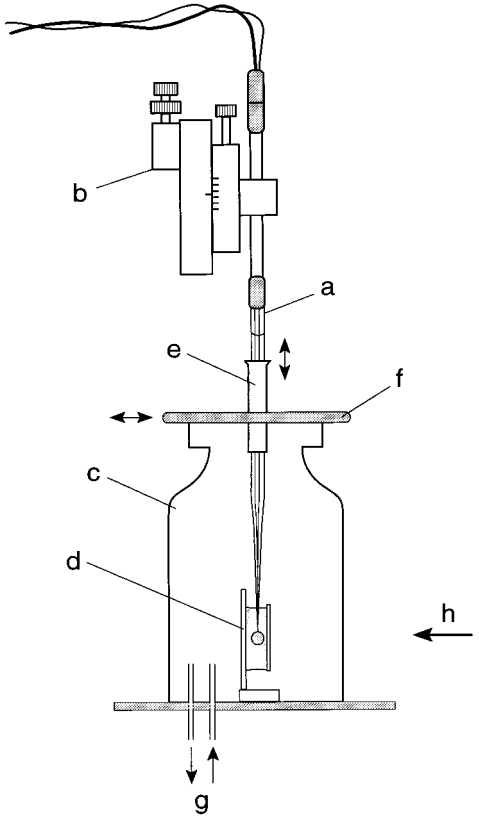

FIG. 3. Experimental setup used for microelectrode measurements in termite guts under defined atmospheres. The microelectrode (a) was attached to a micromanipulator (b) and inserted into a glass bell (c) containing the microchamber (d) with the agarose-embedded gut. The microelectrode could be positioned both vertically within the shaft (e) and laterally together with the cover (f). The headspace within the glass bell was flushed with gas mixtures of various compositions (g). The arrow (h) indicates the angle of view with the dissecting microscope. For more details, see Materials and Methods.

only slightly larger than the outer diameter of the microelectrode shaft, through which the microelectrode was inserted into the bell. A seal was formed by a thin film of silicone oil applied to all movable parts. With this device, the microelectrode tip could be positioned vertically and laterally within the bell while the headspace of the bell was continuously flushed with the desired gas mixture. Flow rates were 2 ml/s, and the back pressure created at the outlet was negligible. The entire setup is depicted diagrammatically in Fig. 3.

All microelectrodes were positioned with a manual micromanipulator (MM33; Märzhäuser, Wetzlar, Germany). In practice, the minimum step increment used was 20 μm; progress of the tip was observed with a horizontally mounted stereomicroscope. Usually, the fine microelectrode tip caused only a small deformation (20 to 50 μm) of the gut wall before penetration. This could not be avoided, and since the deformed gut wall rebounded after it was punctured with the electrode, only negligible bias of the actual position of the electrode tip relative to the gut wall was created. All measurements were done at room temperature (20 to 22 °C).

Redox microelectrodes. A platinum wire (0.1-mm diameter, 99.99% purity; Degussa, Hanau, Germany) was tapered at one end by etching in a saturated aqueous KCN solution to a tip diameter of about 10 μm, cleaned, and inserted into a suitable capillary drawn from green diode glass (Reed glass 8512; Schott, Landshut, Germany), which was then annealed with the platinum in an electrically heated "microforge" as described by Revsbech and Jørgensen (33). The electrode was fused to a shaft and inserted into a glass casing formed from a drawn Pasteur pipette with the platinum tip protruding about 1 mm and fixed with a drop of fast-curing epoxy glue. The outer casing was filled with 1 M KCl, fitted with a chlorinated silver wire for ground connection for electrical shielding (20), and then sealed with epoxy glue. The procedure is similar to the respective steps in the construction of the Clark-type microelectrodes, but the platinum tip and the glass coat were made sturdier, since the tip is not protected by the outer casing. Connection of the working electrode to a high-impedance amplifier electrometer ($R_i \geq 10^{14}$ Ω) was achieved via a low-noise coaxial cable. Electrode potentials were measured against a saturated calomel electrode (Ref 401; Radiometer, Copenhagen, Denmark) which was in contact with the agarose-filled microchamber via a KCl-filled agar bridge. Reference and casing were grounded. Redox electrodes were tested and calibrated with a saturated quinhydrone solution made up with commercial pH calibration standards (pH 4.0 to 7.0).

Measurement of respiratory gas exchange with live termites. About 10 to 20 termites were taken from the nest and placed into a 5-ml glass vial stoppered with a rubber septum. When indicated, the gas headspace was exchanged by flushing with N_2 or by the addition of known quantities of H_2. Headspace samples were taken with a syringe equipped with a gas-tight valve. Separations were performed by gas chromatography on a molecular sieve column; H_2 and CO concentrations were measured with an HgO-reduction trace gas analyzer (13), CH_4 was measured by flame ionization detection (29). The results of repetitive experiments were consistent and indicated that variations among the individual termites were sufficiently eliminated.

RESULTS

Axial profiles of hydrogen, oxygen, and redox potential. From a previous study, we knew that freshly prepared termite guts embedded in agarose-solidified Ringer's solution remain physiologically active for 30 to 60 min (as indicated by gut peristalsis) and generate a steady-state oxygen gradient in the microchamber within 10 min after embedding (6). The results obtained in the experiments reported here confirmed these observations and allowed them to be extended to the hydrogen concentration gradients and gut redox potentials.

The first measurements already showed an unexpectedly high accumulation of H_2 within the gut lumen of *R. flavipes*. Axial profiles of H_2 concentration, measured at the gut center, revealed that the highest values were present in the anterior paunch, whereas they were typically low in the midgut and colon (Fig. 4A). Apart from the paunch, only the rectal dilatation, and this only when the feces were not voided during dissection, gave rise to H_2 concentrations exceeding those of the nondilated regions of the intestinal tract. When the measurements were performed under N_2, the H_2 partial pressure in the paunch increased more than twofold (Fig. 4A).

Axial redox potential profiles (Fig. 4B) basically followed the shape of the corresponding O_2 profiles. High H_2 partial pressures appeared to be strictly correlated with both low redox potential (around or slightly below −200 mV) and with anoxia, since these conditions were established only in the paunch and never in any undilated gut region. The rectal dilation was found to be anoxic only in the rare cases when the rectum remained completely filled during gut preparation; accordingly, the data points pertaining to this gut region are not very reliable.

Radial profiles of hydrogen and oxygen. Figure 5 shows a typical set of radial profiles of the oxygen and hydrogen partial pressures in the anterior paunch of *R. flavipes* incubated under air. O_2 decreased almost linearly from the agarose surface towards the gut, penetrated into the gut lumen, and was completely consumed within a depth of 20 to 200 μm below the gut wall. Such profiles are in good agreement with previous results obtained for these and other termites (6). H_2 concentrations, however, were always highest at the gut center and decreased steeply towards the gut periphery. The curvature of the concentration profiles indicated the presence of H_2-producing activities within the lumen and H_2-consuming activities towards the gut periphery. Notably, at least part of the H_2 consumption zone falls within the microoxic region at the epithelium. In most cases, residual H_2 at the gut wall gave rise to a diffusive flux of H_2 through the agarose overlay towards the atmosphere.

It should be emphasized that the graphs presented here are typical examples of many similar profiles obtained from dozens of separate experiments with different guts. Whereas the shapes of the profiles were similar in all cases, there was considerable variability regarding the absolute H_2 concentrations

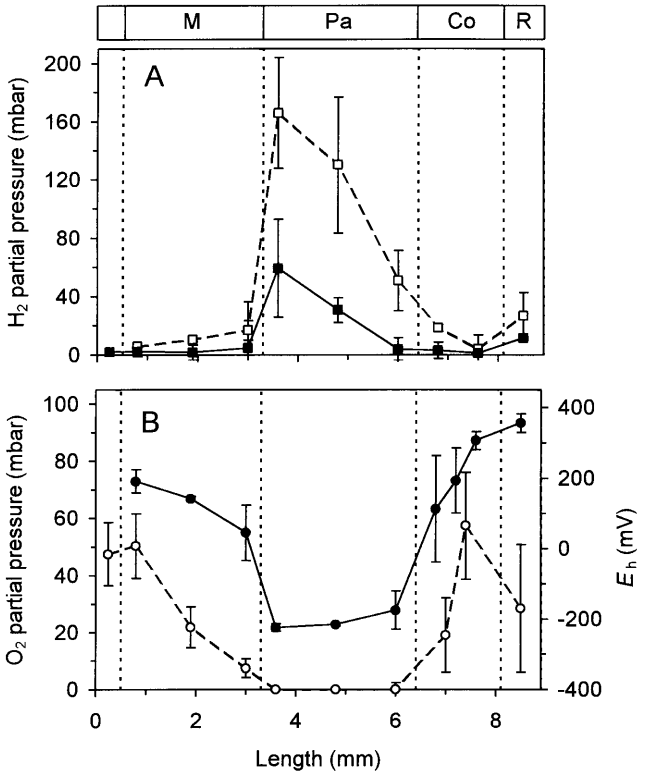

FIG. 4. Axial profiles of hydrogen, oxygen, and redox potential in guts of *R. flavipes* embedded in agarose-solidified Ringer's solution. (A) H_2 partial pressures were determined both under air (■) and under N_2 (□); (B) O_2 partial pressure (○) and redox potential (●) were measured under air. Values are averages (±SDs) of five independent profiles (10 profiles for O_2). Gut regions are indicated by vertical dotted lines. M, midgut; Pa, paunch; Co, colon; R, rectum. 1 mbar = 0.1 kPa.

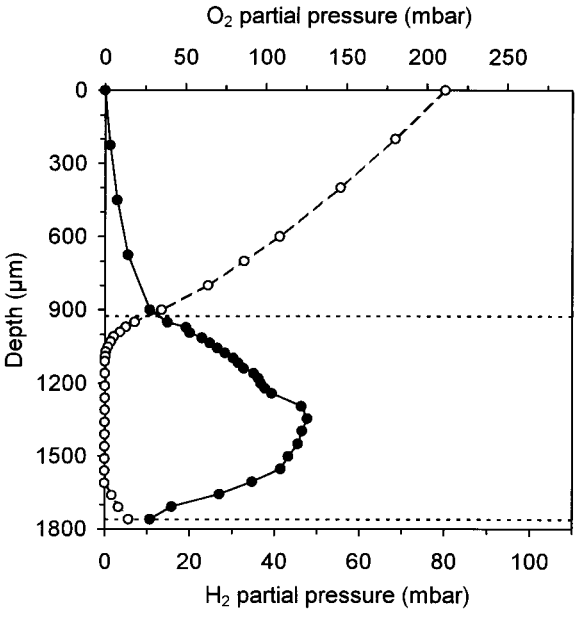

FIG. 5. Typical radial profiles of O_2 (○) and H_2 (●) partial pressures in the anterior paunch of *R. flavipes* (1 mbar = 0.1 kPa). Guts were embedded in agarose-solidified Ringer's solution; the depth scale starts at the agarose surface. The dotted lines in the middle and at the bottom of the graph indicate the positions of the proximal and the distal gut wall, respectively. The measurements were done under air.

measured at the center of the paunch (Table 1). Typically, luminal H_2 was not completely consumed within the gut, but in some cases, it was efficiently removed before it reached the gut wall. Interestingly, this occurred particularly with the guts that exhibited the highest respiratory activities and consumed O_2 so rapidly that it sometimes was not detectable about 20 µm below the gut wall, which was within the resolution limit of the experimental setup.

Effects of increased hydrogen partial pressure. In order to test the possible participation of O_2 in the H_2-consuming processes at the gut periphery, it was necessary to perform measurements under controlled gas headspace. Using the experimental device depicted in Fig. 3, we were able to flush the headspace above the microchamber with any desired mixture of air, N_2, H_2, and O_2. Figure 6 shows typical examples of the H_2 profiles obtained under such conditions. Under an N_2 headspace, the H_2 concentration in the anterior paunch increased significantly (Fig. 6A), often more than threefold (Table 1). Nevertheless, there was always a steep H_2 gradient towards the gut wall, indicating the presence of anaerobic, H_2-consuming activities in the gut periphery. The concentration of the residual H_2 at the gut wall was slightly higher under anoxic than under oxic conditions, and consequently, the first-order diffusive flux of H_2 from gut to atmosphere increased.

However, if an excess of external H_2 (20 kPa) was supplied via the headspace gas, either in the presence or in the absence of O_2, the H_2 flux in the agarose overlay was inverted, since the gut wall now acted as a sink for both the externally supplied and the internally produced H_2 (Fig. 6B). Diffusive flux of H_2 into the gut was significantly lower in the absence than in the presence of O_2. This is not necessarily indicative of an aerobic oxidation of H_2 but can be explained by a partial saturation of the H_2-consuming activities by endogenously produced H_2, which accumulated to higher concentrations under anoxic than under oxic conditions. Accordingly, the highest luminal H_2 partial pressures were observed under anoxic conditions when a simultaneous supply of external H_2 was provided. The influence of various headspace gas mixtures on the absolute values of H_2 accumulation in the anterior paunch region of the hindgut is summarized in Table 1.

It may be significant that the curvature of most of the profiles measured showed two distinct regions of H_2 consumption, one located right below the gut epithelium and one more towards the gut center; this phenomenon was most obvious with the profiles obtained under anoxic conditions (Fig. 6). In addition, the radial asymmetry in most H_2 profiles appeared to be significant. It was not caused by the small but unavoidable differences in the thickness of the agarose layers above and

TABLE 1. Influence of gas headspace on H_2 partial pressures and the corresponding steady-state H_2 concentrations at the center of the anterior paunch of *R. flavipes* guts embedded in agarose[a]

Headspace gas	H_2 partial pressure (kPa)	H_2 concentration (µmol liter^{-1})	*n*
Air	4.9 ± 1.5	39 ± 12	15
N_2	16.5 ± 5.6	131 ± 44	8
Air + H_2[b]	8.1 ± 3.4	64 ± 27	7
N_2 + H_2[b]	27.3 ± 11	217 ± 87	8

[a] Experimental conditions were the same as those shown in Fig. 6. All values are averages ± SDs of *n* independent measurements.
[b] Headspace H_2 partial pressure of 20 kPa.

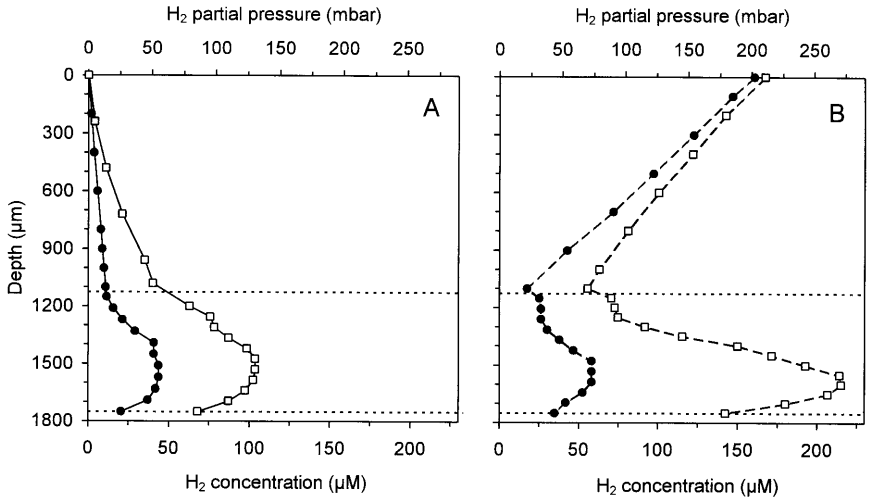

FIG. 6. Effect of gas headspace composition on radial profiles of H_2 partial pressure in the anterior paunch of *R. flavipes*. (A) The measurements shown were performed under a headspace of air (●) or N_2 (□) with the experimental setup shown in Fig. 3. (B) The respective headspaces were supplemented with 20 kPa of H_2 (1 mbar = 0.1 kPa). For further details, refer to the legend for Fig. 5.

below the gut and may well reflect an inhomogeneous distribution of microorganisms within the hindgut, which itself is far from symmetrical.

Effects of increased oxygen partial pressure and defaunation. When the O_2 partial pressure of the gas headspace was increased above ambient, O_2 penetrated deeper into the lumen, rendering it completely oxic at headspace partial pressures between 25 and 30 kPa, depending on the depth of embedding (Fig. 7A). Under such conditions, H_2 no longer accumulated in the hindgut (Fig. 7B); the slightly positive readings are artifacts caused by the baseline shifts due to the residual O_2 sensitivity of that particular electrode which was not subtracted. When external H_2 was added under conditions in which no internal H_2 was produced, the concentration profiles revealed the presence of two distinct regions with different H_2-consuming activities (Fig. 7B). The shape of this curve bears an interesting resemblance to the asymmetry observed in the profiles under H_2-producing conditions.

When *R. flavipes* workers were defaunated by hyperbaric oxygen treatment and fed a diet of starch, all the larger, cellulolytic flagellates disappeared from the hindgut. Such guts no longer accumulated any H_2 within the lumen under oxic or anoxic conditions and no longer acted as a sink for externally supplied H_2 (not shown).

Respiration measurements. Since there are good reasons to assume that H_2 consumption at the gut wall is caused at least partially by the activity of methanogens residing on the gut epithelium (23), we tested the influence of the headspace gas composition on H_2 and CH_4 emission by live termites (Fig. 8). When groups of 10 to 20 termites were incubated in small glass vials under air, they emitted H_2 at a rate of 163 ± 90 nmol (g of termite)$^{-1}$ h^{-1} (n = 4), a rate which is less than 0.5% of the respiratory O_2 consumption. Under anoxic conditions, the H_2 formation rate increased only 1.5-fold, implying that the H_2-consuming activity at the gut epithelium was an O_2-independent process. CH_4 formation rates, which were in the same range as those of H_2, were affected even less.

The situation changed when headspace H_2 partial pressure was increased. Even at 0.1 kPa of H_2, the termites acted as H_2 sinks under oxic and anoxic conditions, and CH_4 production rates increased about twofold over the rate observed without the addition of H_2 (Fig. 8). Under a headspace of 20 kPa of H_2,

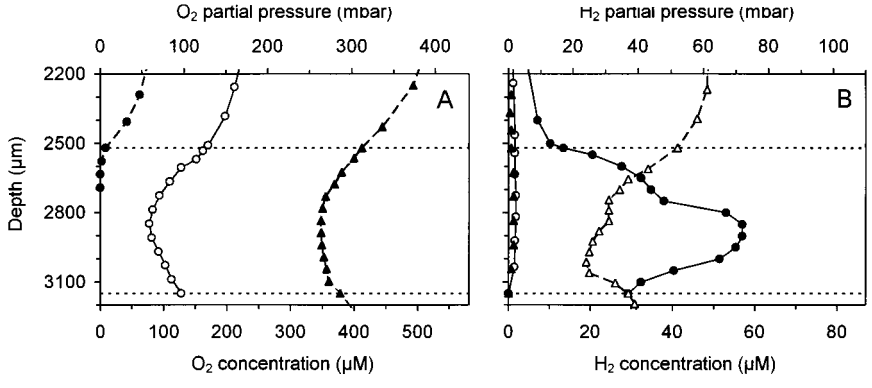

FIG. 7. Influence of hyperatmospheric oxygen partial pressures (1 mbar = 0.1 kPa) on the radial profiles of oxygen (A) and hydrogen (B) partial pressure in the anterior paunch of *R. flavipes*. All measurements were performed under a defined gas headspace consisting of air (●), 30 kPa of O_2 in N_2 (○), 30 kPa of O_2 + 10 kPa of H_2 in N_2 (△), and 50 kPa of O_2 in N_2 (▲) with the experimental setup shown in Fig. 3. Since the guts were embedded relatively deep, only part of the agarose overlay is shown. For further details, refer to the legend for Fig. 5.

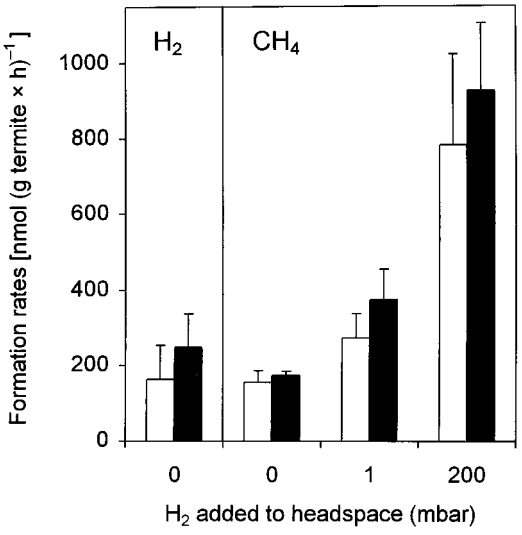

FIG. 8. Hydrogen and methane formation by live termites (groups of 10 to 20 workers) during short-term incubation (0.5 to 1 h) in stoppered glass vials. The gas headspace consisted of air (open bars) or N_2 (closed bars), sometimes amended with H_2 at the indicated partial pressures (1 mbar = 0.1 kPa). Averages and SDs of four independent experiments are given.

CH_4 formation rates were five- to sixfold higher than in the absence of an external H_2 supply and amounted to about 5% of the termites' respiratory O_2 consumption. The small differences between CH_4 emission in the presence and absence of oxygen indicate that O_2-dependent CH_4 oxidation, if it occurs, is not a quantitatively significant process.

Besides H_2 and CH_4, the live *R. flavipes* also emitted small amounts of CO. The initial rates were roughly 15 to 30 nmol (g of termite)$^{-1}$ h^{-1} but declined rapidly (within minutes); the headspace CO partial pressure never exceeded 0.3 to 0.4 Pa.

DISCUSSION

Clark-type polarographic oxygen microelectrodes were introduced to microbial ecology by Revsbech and coworkers more than a decade ago and have proved to be invaluable for the investigation of respiratory and photosynthetic processes in small, structured ecosystems like microbial mats and sediments (32). Polarographic hydrogen measurements, however, are quite rare, since H_2, unlike O_2, usually does not accumulate to partial pressures which are within the dynamic range of such electrodes. So far, the only study involving microelectrodes is that by Witty (38), who measured nodular H_2 production and uptake in leguminous plants.

This is the first description of H_2 microgradients at the oxic-anoxic interface of a small, microbially dominated ecosystem. We were able to employ polarographic microsensors because the H_2 partial pressures in the hindgut lumen of *R. flavipes* were typically very high (ca. 5 kPa), exceeding the values encountered in freshwater sediments (1 to 10 Pa [10, 22]) by more than 3 orders of magnitude. Such high values resemble certain postfeeding situations in the rumen, in which H_2 partial pressures around 2 kPa were recorded (35), but are quite unexpected in a termite that is known to emit only small amounts of H_2. However, the high spatial resolution of the microsensors allowed us to demonstrate the existence of steep H_2 gradients from the gut center towards the epithelium. The gradient curvature indicated the presence of large H_2-consuming activities within the gut periphery and thus reconciles the presence of extremely high intestinal H_2 partial pressures with an only moderate, but significant leakage of this gas through the gut epithelium via the tracheal system to the atmosphere.

These findings necessitate another change in the general concept of hydrogen metabolism in termite hindguts. In his studies on termites of the genus *Zootermopsis* more than 50 years ago, Hungate (17) recognized that H_2 is a major fermentation product of the large, cellulolytic flagellates found in the hindguts of all lower termites. Since then, termite gut protozoa have been studied taxonomically (16), but knowledge of their physiology is still extremely poor, mainly because only a few species have been isolated in pure culture (for a review, see reference 2). Odelson and Breznak (28) demonstrated that axenic cultures of *Trichomitopsis termopsidis*, a trichomonad flagellate from *Zootermopsis angusticollis*, fermented cellulose to hydrogen and acetate (and CO_2) as the only detectable fermentation products, with final H_2-to-acetate ratios of approximately 2:1. Ignoring the fact that the protozoa were grown in a complex medium containing heat-killed *Bacteroides* sp. and fetal bovine serum, and assuming that mainly hexoses were fermented, one arrives at the following idealized equation:

$$<C_6H_{12}O_6> + 2H_2O \rightarrow 2CH_3COO^- + 2H^+ + 2CO_2 + 4H_2 \quad (1)$$

The importance of hydrogen as a major product of termite hindgut fermentation is obvious, but if this reaction were predominant among the termite gut microbiota, termites would release four molecules of H_2 for every hexose equivalent degraded. The H_2 formation rates of living termites, however, are much lower than the corresponding cellulose degradation rates that can be estimated from the animals' respiratory O_2 consumption (27). Breznak and coworkers (1, 5, 27) discovered that homoacetogenesis and methanogenesis play an important role in reoxidation of the H_2 formed by the microbial fermentations in the termite hindgut. The same activities are typical for anoxic freshwater ecosystems, where, depending on particular environmental parameters, one process usually outcompetes the other (34). Almost all termites tested, however, simultaneously emit significant amounts of methane and exhibit H_2-CO_2 homoacetogenesis in their hindgut homogenates, albeit at varying ratios (1). Whereas termites from certain (sub) families are largely "methanogenic," others possess higher activities of H_2-CO_2-dependent homoacetogenesis (1). The simultaneous presence and especially this apparent outcompetition of methanogens by homoacetogens in termite hindguts are quite enigmatic. Breznak (3) summarized several possible scenarios which might serve as an explanation and which range from a lowered hydrogen threshold of homoacetogens under mixotrophic conditions to a close, possibly intracellular association of the homoacetogens with the H_2-producing protozoa. All of these models, however, assume that hydrogen concentrations within the gut must be relatively low.

The microelectrode profiles presented here show that this is definitely not the case. Hydrogen accumulation is strongest within the anterior hindgut of *R. flavipes*, a finding which is in agreement with the location of the cellulolytic protozoa and the large pools of acetate within this region (27) and which is additionally supported by the strict correlation between hydrogen formation, anoxia, and a low redox potential (≤ -200 mV) in the axial profiles (Fig. 4). We demonstrated that the coincidence of these parameters is governed by a fine-tuned equilibrium of the diffusive influx of oxygen and its removal by the respiratory activity of the hindgut microbiota, which can be easily disturbed if, e.g., the oxygen partial pressure around the

gut is increased. In that case, the diffusive flux of oxygen increases, and oxygen penetrates deeper into the lumen. When the influx of oxygen surpasses the oxidative capacities of the gut microbiota, the gut becomes completely oxic, and luminal production of hydrogen ceases (Fig. 7). Prolonged exposure of the hindgut microbiota to large oxygen partial pressures appears to be deleterious to the protozoa and probably also to the H_2-consuming anaerobic bacteria, as the results of the defaunation experiment indicate. Termites treated with hyperbaric oxygen for several hours not only lost their protozoa and no longer showed any H_2 accumulation, but in contrast to the guts exposed only to slightly elevated oxygen partial pressures, also completely lost all H_2-consuming activities.

Hindguts were embedded in agarose to prevent their otherwise rapid desiccation during the measurements and to stabilize any diffusion gradients around the hindgut proper. These experimental conditions may not exactly reflect the situation in the living termite; however, there are valid reasons for assuming that they are not too different. The results discussed in the preceding paragraph indicate that the in situ oxygen concentration at the gut epithelium cannot significantly exceed that encountered under experimental conditions—or the hindguts would be completely oxic. On the other hand, it is extremely unlikely that the epithelial oxygen supply of living termites is much lower than that under experimental conditions. The tracheal system of the termite directly connects individual cells of the gut epithelium with the surrounding atmosphere, allowing diffusive transport to occur almost exclusively within the gaseous phase, and should represent a smaller diffusion barrier than that imposed by 1 to 2 mm of aqueous agarose.

Our results clearly demonstrate the existence of a most active site of H_2 oxidation right at the gut epithelium and the existence of a second one more towards the center (Fig. 6). Since this H_2 sink is present under both oxic and anoxic conditions, it must be attributed to hydrogenotrophic anaerobes. It is surprising that despite the location of this region within the microoxic zone directly below the gut wall, and despite the presence of significant numbers of potentially H_2-oxidizing aerobic bacteria in *R. flavipes* hindguts (36), anaerobic microorganisms seem to be the major hydrogen consumers. Recently, Leadbetter and Breznak (23) reported that the gut of *R. flavipes* contains large numbers of methanogens of the genus *Methanobrevibacter* and that most of the methanogenic population resides directly on the luminal side of the gut epithelium. According to our oxygen microsensor studies, this places them directly within the microoxic periphery of the hindgut, where they are exposed to the highest O_2 concentrations encountered within the gut.

Collectively, our results and those of Leadbetter and Breznak (23) substantiate the hypothesis that the coexistence of both homoacetogens and methanogens in the hindgut is not a question of direct competition for a mutual resource, but, rather, a resource partitioning effected by the spatial distribution of the different hydrogen-consuming populations within the gut. While the homoacetogens may be located more towards the hindgut lumen, where H_2 is provided in excess, the methanogens apparently reside in the periphery and scavenge their share of this substrate while the rest leaves the gut via the tracheal system into the atmosphere. The escape of H_2 from the gut may be due also to a certain degree of patchiness observed in epithelium colonization by methanogens (23). In the respiration experiments, live termites were found to emit CO at low rates, which were apparently compensated for by CO consumption as soon as the partial pressure reached 0.3 to 0.4 Pa. It is not possible at this point to attribute this activity to homoacetogenic or methanogenic members of the gut microflora. Dissolved CO was also reported previously to accumulate in freshwater sediments to concentrations around 5 to 20 nM (22).

How important is methanogenesis as an H_2 sink in *R. flavipes*? After all, live *R. flavipes* emit only small amounts of methane (0.155 μmol of CH_4 [g of termite]$^{-1}$ h^{-1} [this paper; see also reference 27]), whereas their gut homogenates show high activities of H_2-CO_2 homoacetogenesis (1.11 μmol of acetate [g of termite]$^{-1}$ h^{-1} 5). The rates for both processes are not directly comparable, since methane formation was measured under in vivo conditions, whereas the value for homoacetogenesis represents only a potential rate determined in gut homogenates under H_2 saturation. If external H_2 is supplied to live termites via the gas phase, rates of methanogenesis increase five- to sixfold to almost 1 μmol [g of termite]$^{-1}$ h^{-1} (Fig. 8), which is close to the value for H_2-CO_2-dependent acetogenesis found in gut homogenates.

To compare this rate to the H_2 uptake rates of agarose-embedded guts incubated under H_2 (Fig. 6), we approximated the hindgut as an endless cylinder and estimated the H_2 flux into the gut, using Fick's first law of diffusion: $J = -2\pi r\, l\, \phi\, D_s\, \delta C(r)/\delta r$ (11), where J is the total flux of molecules through the paunch surface per unit of time, r and l are paunch radius and length, ϕ is the porosity of the agarose, D_s is the apparent diffusion coefficient, and $\delta C(r)/\delta r$ is the slope of the concentration gradient at radius r. For the porosity and the H_2 diffusion coefficient, we used the values for pure water ($\phi = 1$; $D_s = 3.81 \times 10^{-9}$ m^2 s^{-1} at 21°C [14]), which, in the case of oxygen, have been found to be applicable at agar concentrations up to 2% and over a wide range of salinity values (31). From the experimental data, we determined the average slope of the H_2 diffusion gradients directly above the gut as (-22.6 ± 3.2) kPa mm^{-1} ($n = 6$), which can be converted to -182 μmol liter^{-1} mm^{-1}, using the solubility of H_2 of 18.2 ml (s.t.p.) liter^{-1} atm^{-1} at 20°C (25). Given the average dimensions of the paunch ($r = 0.4$ mm; $l = 2$ mm), the calculation yields an H_2 influx of 3.47×10^{-12} mol s^{-1}, which is equivalent to 2.50 μmol (g of termite)$^{-1}$ h^{-1}. This means that the estimated H_2 consumption of agarose-embedded guts would account for more than half of the CH_4 formed by living termites under comparable conditions.

Messer and Lee (26) reported that externally supplied H_2 induced a strong increase in CH_4 formation by live *Z. angusticollis*. These researchers followed up on the observation of Lee et al. (24) that *Z. angusticollis* harbors intestinal protozoa which are closely associated with fluorescent methanogens. In *R. flavipes*, however, virtually all fluorescent methanogens were either directly attached to or associated with the gut wall (23). It is not clear whether Lee et al. checked for fluorescent cells attached to the gut wall in *Z. angusticollis*; accordingly, we can only speculate whether the situation in this termite is different from that in *R. flavipes*. After all, *Z. angusticollis* reportedly emits much more CH_4 per unit time than *R. flavipes* (1). The possibility that in *R. flavipes* the homoacetogens rather than the methanogens might be associated with the protozoa has been mentioned previously (4).

From the results shown in Fig. 6 and 7, it is obvious that the presence of O_2 has a significant impact on the luminal hydrogen concentrations, which can be explained either by a direct oxidation of H_2 with O_2 or by an indirect effect of O_2 on the fermentation product pattern of the gut microbiota. In a recent study, we were able to show that O_2 has a strong influence on the metabolic product pattern of the numerically dominant population of lactic acid bacteria in the *R. flavipes* hindgut (36). This may also be true for termite gut protozoa, since similar shifts in fermentation product patterns in the presence of low

O_2 partial pressures were also reported for "anaerobic" rumen ciliates (12). After all, a metabolism according to equation 1 is quite problematic at high H_2 partial pressures. The overall free energy change of the reaction is exergonic ($\Delta G^{o\prime} = -199$ kJ/mol of reaction), but since the underlying pathway most probably involves glucose fermentation via glyceraldehyde-phosphate dehydrogenase and pyruvate-ferredoxin oxidoreductase, the formation of H_2 via reduced pyridine nucleotides generated in the former reaction is rendered thermodynamically unfavorable at H_2 partial pressures above 0.1 kPa (34). Since low luminal hydrogen partial pressures can now be ruled out, the overall reaction may proceed only if the protozoa possess a reverse electron transport mechanism to shift the reducing equivalents from pyridine nucleotides to a more negative acceptor, e.g., ferredoxin. Alternatively, the reaction stoichiometry in situ may differ from that given in equation 1, e.g., substituting H_2 formation with that of more reduced fermentation products (e.g., propionate or butyrate) or involving O_2 as a terminal electron acceptor. We are currently trying to investigate the role of O_2 in hindgut carbon and electron flow in *R. flavipes* with radiotracer techniques.

In summary, the present study provides strong support for the emerging concept that termite hindguts are not homogeneous anoxic fermenters but highly structured systems with steep gradients of metabolites (6, 8) and pH (7).

ACKNOWLEDGMENTS

This study was supported by a grant from the Deutsche Forschungsgemeinschaft (DFG) to A.B. within the program Structural and Functional Analysis of Natural Microbial Communities.

We thank Bernhard Schink for his support and stimulating discussions and John Breznak and David Emerson for critically reading a previous version of the manuscript.

REFERENCES

1. **Brauman, A., M. D. Kane, M. Labat, and J. A. Breznak.** 1992. Genesis of acetate and methane by gut bacteria of nutritionally diverse termites. Science **257:**1384–1387.
2. **Breznak, J. A.** 1982. Intestinal microbiota of termites and other xylophagous insects. Annu. Rev. Microbiol. **36:**323–343.
3. **Breznak, J. A.** 1994. Acetogenesis from carbon dioxide in termite guts, p. 303–330. *In* H. L. Drake (ed.), Acetogenesis. Chapman and Hall, New York, N.Y.
4. **Breznak, J. A., and A. Brune.** 1994. Role of microorganisms in the digestion of lignocellulose by termites. Annu. Rev. Entomol. **39:**453–487.
5. **Breznak, J. A., and J. M. Switzer.** 1986. Acetate synthesis from H_2 plus CO_2 by termite gut microbes. Appl. Environ. Microbiol. **52:**623–630.
6. **Brune, A., D. Emerson, and J. A. Breznak.** 1995. The termite gut microflora as an oxygen sink: microelectrode determination of oxygen and pH gradients in guts of lower and higher termites. Appl. Environ. Microbiol. **61:**2681–2687.
7. **Brune, A., and M. Kühl.** 1996. pH profiles of the extremely alkaline hindguts of soil-feeding termites (Isoptera: Termitidae) determined with microelectrodes. J. Insect Physiol. **42:**1121–1127.
8. **Brune, A., E. Miambi, and J. A. Breznak.** 1995. Roles of oxygen and the intestinal microflora in the metabolism of lignin-derived phenylpropanoids and other monoaromatic compounds by termites. Appl. Environ. Microbiol. **61:**2688–2695.
9. **Cleveland, L. R.** 1926. Symbiosis among animals with special reference to termites and their intestinal flagellates. Q. Rev. Biol. **1:**51–64.
10. **Conrad, R.** 1995. Soil microbial processes involved in production and consumption of atmospheric trace gases, p. 207–250. *In* J. G. Jones (ed.), Advances in microbial ecology, vol. 14. Plenum Press, New York, N.Y.
11. **Crank, J.** 1975. The mathematics of diffusion, 2nd ed. Clarendon Press, Oxford, United Kingdom.
12. **Ellis, J. E., P. S. McIntyre, M. Saleh, A. G. Williams, and D. Lloyd.** 1991. Influence of CO_2 and low concentrations of O_2 on fermentative metabolism of the ruminal ciliate *Polyplastron multivesiculatum*. Appl. Environ. Microbiol. **57:**1400–1407.
13. **Friedrich, M., and B. Schink.** 1993. Hydrogen formation from glycolate driven by reversed electron transport in membrane vesicles of a syntrophic glycolate-oxidizing bacterium. Eur. J. Biochem. **217:**233–240.
14. **Gertz, K. H., and H. H. Loeschcke.** 1954. Bestimmung des Diffusionskoeffizienten von H_2, O_2, N_2, und He in Wasser und Blutserum bei konstant gehaltener Konvektion. Z. Naturforsch. Teil B **9:**1–9.
15. **Gilman, S.** 1967. The anodic film on platinum electrodes, p. 111–192. *In* A. J. Bard (ed.), Electroanalytical chemistry, vol. 2. Marcel Dekker, New York, N.Y.
16. **Honigberg, B. M.** 1969. Protozoa associated with termites and their role in digestion, p. 1–36. *In* K. Krishna and F. M. Weesner (ed.), Biology of termites, vol. 2. Academic Press, New York, N.Y.
17. **Hungate, R. E.** 1939. Experiments on the nutrition of *Zootermopsis*. III. The anaerobic carbohydrate dissimilation by the intestinal protozoa. Ecology **20:**230–245.
18. **Hungate, R. E.** 1943. Quantitative analyses of the cellulose fermentation by termite protozoa. Ann. Entomol. Soc. Am. **36:**730–739.
19. **Hungate, R. E.** 1955. Mutualistic intestinal protozoa, p. 159–199. *In* S. H. Hutner and A. Lwoff (ed.), Biochemistry and physiology of protozoa, vol. 2. Academic Press, New York, N.Y.
20. **Jensen, K., N. P. Revsbech, and L. P. Nielsen.** 1993. Microscale distribution of nitrification activity in sediment determined with a shielded microsensor for nitrate. Appl. Environ. Microbiol. **59:**3287–3296.
21. **Jones, J. W., and N. I. Bishop.** 1976. Simultaneous measurement of oxygen and hydrogen exchange from the blue-green alga *Anabaena*. Plant Physiol. **57:**659–665.
22. **Krämer, H., and R. Conrad.** 1993. Measurement of dissolved H_2 concentrations in methanogenic environments with a gas diffusion probe. FEMS Microbiol. Ecol. **12:**149–158.
23. **Leadbetter, J. R., and J. A. Breznak.** 1996. Physiological ecology of *Methanobrevibacter cuticularis* sp. nov. and *Methanobrevibacter curvatus* sp. nov., isolated from the hindgut of the termite *Reticulitermes flavipes*. Appl. Environ. Microbiol. **62:**3620–3631.
24. **Lee, M. J., P. J. Schreurs, A. C. Messer, and S. H. Zinder.** 1987. Associations of methanogenic bacteria with flagellated protozoa from a termite hindgut. Curr. Microbiol. **15:**337–341.
25. **May, A.** 1967. Löslichkeit von Gasen in Flüssigkeiten, p. 1203–1232. *In* E. Lax (ed.), D'Ans · Lax, Taschenbuch für Chemiker und Physiker, 3rd ed., vol. 1. Springer Verlag, Berlin, Germany.
26. **Messer, A. C., and M. J. Lee.** 1989. Effect of chemical treatments on methane emission by the hindgut microbiota in the termite *Zootermopsis angusticollis*. Microb. Ecol. **18:**275–284.
27. **Odelson, D. A., and J. A. Breznak.** 1983. Volatile fatty acid production by the hindgut microbiota of xylophagous termites. Appl. Environ. Microbiol. **45:**1602–1613.
28. **Odelson, D. A., and J. A. Breznak.** 1985. Nutrition and growth characteristics of *Trichomitopsis termopsidis*, a cellulolytic protozoan from termites. Appl. Environ. Microbiol. **49:**614–621.
29. **Platen, H., and B. Schink.** 1987. Methanogenic degradation of acetone by an enrichment culture. Arch. Microbiol. **149:**136–141.
30. **Revsbech, N. P.** 1989. An oxygen microelectrode with a guard cathode. Limnol. Oceanogr. **34:**472–476.
31. **Revsbech, N. P.** 1989. Diffusion characteristics of microbial communities determined by use of oxygen microsensors. J. Microbiol. Methods **9:**111–122.
32. **Revsbech, N. P.** 1994. Analysis of microbial mats by use of electrochemical microsensors: recent advances, p. 135–147. *In* L. J. Stahl and P. Caumette (ed.), Microbial mats. Springer Verlag, Berlin, Germany.
33. **Revsbech, N. P., and B. B. Jørgensen.** 1986. Microelectrodes: their use in microbial ecology. Adv. Microb. Ecol. **9:**293–352.
34. **Schink, B.** 1997. Energetics of syntrophic cooperation in methanogenic degradation. Microbiol. Mol. Biol. Rev. **61:**262–280.
35. **Smolenski, W. J., and J. A. Robinson.** 1988. In situ rumen hydrogen concentrations in steers fed eight times daily, measured using a mercury reduction detector. FEMS Microbiol. Ecol. **53:**95–100.
36. **Tholen, A., B. Schink, and A. Brune.** The gut microflora of *Reticulitermes flavipes*, its relation to oxygen, and evidence for oxygen-dependent acetogenesis by the most abundant *Enterococcus* sp. FEMS Microbiol. Ecol., in press.
37. **Wang, R., F. P. Healey, and J. Myers.** 1971. Amperometric measurement of hydrogen evolution in *Chlamydomonas*. Plant Physiol. **48:**108–110.
38. **Witty, J. F.** 1991. Microelectrode measurements of hydrogen concentrations and gradients in legume nodules. J. Exp. Bot. **42:**765–771.